

# Analytic forms for the $e^+e^-$ annihilation cross sections around a resonance including initial state radiation

Baoxin Liu, Zhenyu Zhang,<sup>\*</sup> and Xiang Zhou<sup>†</sup>

*Hubei Nuclear Solid Physics Key Laboratory, School of Physics and Technology,*

*Wuhan University, Wuhan, Hubei 430072, P. R. China*

(Dated: May 16, 2024)

arXiv:2405.09432v1 [hep-ph] 15 May 2024

# Abstract

The exact analytic form of cross sections including initial state radiation with Kuraev-Fadin radiative function are obtained for  $e^+e^-$  annihilation around a resonance. Despite accounting for vacuum polarization and center-of-mass energy spread effects, the precision remains below 0.1%, meeting the accuracy requirements of quantum electrodynamics corrections up to  $\mathcal{O}(\alpha^2)$ . The analytic forms lead to an enhancement in the precision of experimental measurements of physical parameters, such as branching fractions, and demonstrate significantly improved computational efficiency in the regression procedures.

**Keywords:** Initial state radiation, cross section, branching fraction, analytic form.

## I. INTRODUCTION

The  $e^+e^-$  annihilation experiments provide cleaner experimental environments for quarkonium decays than  $p\bar{p}$  and hadron decays experiments. The measured quarkonium decay widths, or the corresponding branching fractions, can serve as inputs in phenomenological models or be used for comparison with theoretical predictions to test our understanding of quantum chromodynamics (QCD) [1]. There is an unavoidable background from the continuum process, which directly produces the final state via  $e^+e^-$  annihilation, i.e.,  $e^+e^- \rightarrow \gamma^* \rightarrow f$  [2]. It has been shown that the cross section from the interference term will lead to imprecise branching fractions for the broad resonance above open heavy flavor threshold, such as  $\psi(3770)$  [3].

A novel study shows that the ratio of the cross section from the interference term with respect to the resonance are surprisingly large compared to the precision of the current experiments even for the narrow resonances below the open heavy flavor threshold, such as  $J/\psi$  and  $\psi(3686)$  [4]. Therefore, to achieve precision measurements of the quarkonium decay widths or the corresponding branching fractions, the cross sections around the resonance at least three energies must be measured [4].

Initial state radiation (ISR) is an essential quantum electrodynamics (QED) correction for the precise measurement of cross sections in  $e^+e^-$  annihilations [5]. In the ISR process,

---

\* zhenyuzhang@whu.edu.cn

† xiangzhou@whu.edu.cn

the electron or positron emits one or more photons before annihilation, thereby reducing the center-of-mass (c.m.) energy. While the Born cross sections of the final state are of interest, it is their corresponding ISR-corrected cross sections that are measured experimentally [6]. The ISR-corrected cross section can be obtained by the structure function (SF) method, which is an integral transformation of the kernel cross section by the radiative function [7]. The SF method, with corrections up to  $\mathcal{O}(\alpha^2)$ , can achieve the required accuracy of about 0.1% for c.m. energy ranging from 0.2 to 10 GeV [7].

The parameters of the Born cross section can be obtained through the integral method and the inverse transformation method. The integral method involves fitting the experimental observed cross sections with the integral of the radiative function multiplied by the model function of Born cross sections [7]. On the other hand, the inverse transformation method utilizes the Born cross section model function to fit the transformed cross sections from the experimental observed ones through an iterative procedure [6, 8] or by solving numerical integral equations [9]. The integral method is straightforward but time-consuming, as it requires numerical integration in the regression iterations [10]. Conversely, the inverse transformation method is time-efficient but introduces an additional uncertainty from the transformation process [6].

For the narrow resonance processes, such as  $J/\psi$  or  $\psi(2S)$ , the widths of the resonances are significantly less than the c.m. energy spread and then the experimental observed cross sections become strongly correlated. Therefore, the parameters of the Born cross section can only be obtained through the integral method [11]. Moreover, the consuming time of the regression process becomes much more burdensome since an additional convolution with the c.m. energy spread must be included in the numerical integration [10].

The integral method will be significantly accelerated if the analytic form of the ISR-corrected cross sections is obtained [10]. The radiative function proposed by Kuraev and Fadin (KF) consists of an exponentiated part and a finite-order leading-logarithmic (LL) part, accounting for soft multi-photon emission and hard collinear bremsstrahlung, respectively [7]. In 1987, R. N. Cahn was the first to derive the analytic form with the exponentiated part in the KF radiative function [12]. The approximate analytic form, including the LL parts in the KF radiative function and the upper limit correction by the exponential expansions, has been developed in subsequent works [10, 11, 13, 14]. However, it is shown below that for the ISR-corrected cross sections around  $J/\psi$ , the accuracy of the approximated

analytic form is within a few percent and propagates in the same order to the estimated value by regression for the hadronic branching fraction. In a sense, the approximated analytic form introduces an imperceptible yet non-negligible systematic uncertainty, which is comparable to the statistical or even the total systematic uncertainty for experiments.

In this paper, we first provide the formalisms of the ISR corrected Born cross sections and validate the precisions in Section II where the formulas of the Born cross sections around a resonance and the corresponding exact analytic forms of the ISR-corrected cross sections incorporating the KF radiative function, referred as the KF analytic forms, are provided in Appendices A and B, respectively. Section III and Section IV introduce the formalisms that incorporate the vacuum polarization effect and the c.m. energy spread effect, respectively, demonstrating the corresponding precisions. The fit tests of the toy Monte Carlo (MC) samples in the vicinity of  $J/\psi$  are presented in Section V. Finally, Section VI gives discussions and conclusions.

## II. ISR CORRECTED BORN CROSS SECTIONS

In the vicinity of a resonance, the amplitude  $A_{\text{tot.}}^f$  of the final state  $f$  in  $e^+e^-$  colliders is the coherent sum of both resonance  $A_R^f$  and continuum amplitudes  $A_C^f$ . The Born cross section can be written as [4]

$$\sigma_{\text{Born}}^f(W) \propto \left| A_{\text{tot.}}^f(W) \right|^2 = \left| A_C^f(W) + A_R^f(W)e^{i\phi} \right|^2, \quad (1)$$

where  $\phi$  is the relative phase between the continuum amplitude  $A_C^f$  and the resonance amplitude  $A_R^f$ . Therefore, the Born cross section is a sum of three parts as

$$\sigma_{\text{Born}}^f(W) = \sigma_{B_C}^f(W) + \sigma_{B_R}^f(W) + \sigma_{B_I}^f(W), \quad (2)$$

where  $\sigma_{B_C}^f(W) \propto \left| A_C^f(W) \right|^2$ ,  $\sigma_{B_R}^f(W) \propto \left| A_R^f(W) \right|^2$  and  $\sigma_{B_I}^f \propto 2\Re\{A_C^f(W)A_R^f(W)\}$  denote the Born cross sections from continuum, resonance and interference contributions, respectively.

When the kernel cross section is the Born cross section, the ISR corrected cross section

$\sigma_{\text{ISR}}^f$  is an integral of the Born cross section  $\sigma_{\text{Born}}^f$  times the radiation function [4], that is

$$\sigma_{\text{ISR}}^f(W) = \int_0^{1 - (\frac{W_{\text{min}}}{W})^2} dx F(x, W) \times \sigma_{\text{Born}}^f(W\sqrt{1-x}), \quad (3)$$

where  $W$  is the c.m. energy of  $e^+e^-$  annihilation and  $W_{\text{min}}$  is the threshold energy equal to the invariant mass of the final states or the experimental cut off energy. The KF radiative function  $F(x, W)$  has the form [7]

$$F(x, W) = x^{\beta-1}(1+\delta) - \beta \left(1 - \frac{x}{2}\right) + \frac{1}{8}\beta^2 [4(2-x) \times \log \frac{1}{x} - \frac{1+3(1-x)^2}{x} \log(1-x) - 6+x], \quad (4)$$

with  $\delta = \frac{3}{4}\beta + \frac{\alpha}{\pi} \left(\frac{\pi^2}{3} - \frac{\pi^2}{12}\right)$  and  $\beta = \frac{2\alpha}{\pi} \left(2 \log \frac{W}{m_e} - 1\right)$ .

The ISR corrected cross section integral  $\sigma_{\text{ISR}}^f$  is a sum of three parts, which is

$$\sigma_{\text{ISR}}^f(W) = \sigma_C^f(W) + \sigma_R^f(W) + \sigma_I^f(W), \quad (5)$$

where

$$\sigma_C^f(W) \equiv \int_0^{1 - (\frac{W_{\text{min}}}{W})^2} dx F(x, W) \sigma_{B_C}^f(W\sqrt{1-x}), \quad (6)$$

$$\sigma_R^f(W) \equiv \int_0^{1 - (\frac{W_{\text{min}}}{W})^2} dx F(x, W) \sigma_{B_R}^f(W\sqrt{1-x}), \quad (7)$$

and

$$\sigma_I^f(W) \equiv \int_0^{1 - (\frac{W_{\text{min}}}{W})^2} dx F(x, W) \sigma_{B_I}^f(W\sqrt{1-x}), \quad (8)$$

are the integrals of the continuum, resonance and interference contributions, respectively.

For the process  $e^+e^- \rightarrow \mu^+\mu^-$  in the vicinity of  $J/\psi$ , the Born cross section is [11]

$$\sigma_{\text{Born}}^{\mu^+\mu^-}(W) = \frac{4\pi\alpha^2}{3W^2} \left| 1 + \frac{W^2}{M} \times \frac{3\sqrt{\Gamma_{ee}\Gamma_{\mu\mu}}}{\alpha(W^2 - M^2 + iM\Gamma)} e^{i\phi} \right|^2, \quad (9)$$

where  $\alpha$  is the fine structure constant,  $M$  and  $\Gamma$  are the mass and total decay width of  $J/\psi$ ,  $\Gamma_{ee}$  and  $\Gamma_{\mu\mu}$  are the decay widths of  $J/\psi \rightarrow e^+e^-$  and  $\mu^+\mu^-$ , respectively. For the processes

$e^+e^- \rightarrow 2(\pi^+\pi^-)\pi^0$  and  $\eta\pi^+\pi^-$  with  $\eta \rightarrow \pi^+\pi^-\pi^0$  in the vicinity of  $J/\psi$ , the Born cross sections can be written in a general form as [11]

$$\sigma_{\text{Born}}^{5\pi}(W) = \left( \frac{\mathcal{A}}{W^2} \right)^2 \frac{4\pi\alpha^2}{3W^2} \left| 1 + \frac{3W^2 \sqrt{\Gamma_{ee}\Gamma_{\mu\mu}} \mathcal{C}_1 e^{i\phi} (1 + \mathcal{C}_2 e^{i\Phi})}{\alpha M (W^2 - M^2 + iM\Gamma)} \right|^2, \quad (10)$$

where  $\frac{\mathcal{A}}{W^2}$  is the form factor,  $\mathcal{C}_1$  and  $\mathcal{C}_2$  are the ratios of amplitudes,  $\Phi$  is the phase between the strong and electromagnetic decays from  $J/\psi$ . For the process of  $e^+e^- \rightarrow 2(\pi^+\pi^-)\pi^0$ ,  $\mathcal{C}_1$  and  $\phi$  are assumed to be 1 and 0, respectively [11].

Therefore, it can be derived for the cross sections from continuum, resonance and interference contributions. For example, the Born cross section from the continuum contribution of  $e^+e^- \rightarrow \mu^+\mu^-$  is

$$\sigma_{BC}^{\mu^+\mu^-}(W) = \frac{4\pi\alpha^2}{3W^2}. \quad (11)$$

The Born cross sections are composed by rational functions, while the KF radiative function contains not only exponential functions but also logarithmic functions, such as  $\log x$ , which make the ISR corrected cross section integral has an integrable singularity at the lower limit  $x = 0$  in Eq. (3). Fortunately, the integral still has an analytic form. For example, the analytic form for the improper integral of  $\log \frac{1}{x}$  times  $\sigma_{BC}^{\mu^+\mu^-}(W)$  is

$$\begin{aligned} \mathcal{I}(W) &= \int_0^{1-\left(\frac{W_{\min}}{W}\right)^2} dx \beta^2 \log \frac{1}{x} \sigma_{BC}^{\mu^+\mu^-}(W\sqrt{1-x}) \\ &= \int_0^{1-\left(\frac{W_{\min}}{W}\right)^2} dx \beta^2 \log \frac{1}{x} \frac{4\pi\alpha^2}{3W^2(1-x)} \\ &= -\beta^2 \frac{4\pi\alpha^2}{3W^2} \int_0^{1-\left(\frac{W_{\min}}{W}\right)^2} dx \frac{\log x}{1-x} \\ &= -\beta^2 \frac{4\pi\alpha^2}{3W^2} \left[ \text{Li}_2\left(\frac{W_{\min}^2}{W^2}\right) - \frac{\pi^2}{6} \right], \end{aligned} \quad (12)$$

where  $\text{Li}_2(x)$  is the Spence's function which is defined as

$$\text{Li}_2(z) = \int_1^{1-z} \frac{\log(x)}{1-x} dx. \quad (13)$$

Since the analytic forms are tedious, we put them into the appendix B.

In Fig. 1, we compare the ISR corrected cross section  $\sigma_{\text{NI}}^{\mu^+\mu^-}$  obtained through the numerical integration (NI) with the KF analytic form  $\sigma_{\text{KF}}^{\mu^+\mu^-}$ , and the approximated analytic form

$\sigma_{\text{Approx}}^{\mu^+\mu^-}$  for the  $e^+e^- \rightarrow \mu^+\mu^-$  process around the  $J/\psi$  resonance. The relative deviation between  $\sigma_{\text{KF}}^{\mu^+\mu^-}$  and  $\sigma_{\text{NI}}^{\mu^+\mu^-}$  is less than  $10^{-10}$ , coinciding with the numerical integration's error tolerance, thereby affirming the precision of our analytic form. Moreover, the relative deviation between  $\sigma_{\text{NI}}^{\mu^+\mu^-}$  and  $\sigma_{\text{Approx}}^{\mu^+\mu^-}$  reaches approximately 0.3% at the incoherent phase  $\phi = 90^\circ$  where  $\sigma_{B_I}^{\mu^+\mu^-}$  and then  $\sigma_I^{\mu^+\mu^-}$  vanish. Therefore, the precision is about 0.3% for the sum of the approximated analytic forms  $\sigma_C^{\mu^+\mu^-}$  and  $\sigma_R^{\mu^+\mu^-}$  where the precision of the approximated analytic form  $\sigma_R^{\mu^+\mu^-}$  is only 0.1% [13]. Conversely, at  $\phi = 0^\circ$  or  $180^\circ$ , the relative deviation between  $\sigma_{\text{NI}}^{\mu^+\mu^-}$  and  $\sigma_{\text{Approx}}^{\mu^+\mu^-}$  is about 3%. It is evident that the deviation comes from  $\sigma_I^{\mu^+\mu^-}$  is 3% in the approximated analytic form.

### III. VACUUM POLARIZATION EFFECT

When the vacuum polarization (VP) effect is considered, the Born cross section in the vicinity of a resonance is corrected as [14, 16]

$$\begin{aligned}\sigma_{\text{Born-VP}}^f(W) &= \sigma_{B_C}^{f\text{VP}}(W) + \sigma_{R_B}^{f\text{VP}}(W) + \sigma_{B_I}^{f\text{VP}}(W) \\ &= \frac{\sigma_{B_C}^f(W)}{|1 - \Pi_0(W)|^2} + \sigma_{B_R}^f(W) \\ &\quad + \frac{\sigma_{B_I}^f(W)}{|1 - \Pi_0(W)|},\end{aligned}\tag{14}$$

where  $\Pi_0(W)$  is the non-resonant VP factor [16].

The ISR corrected cross section with VP effect is also a sum of three parts which is

$$\begin{aligned}\sigma_{\text{ISR-VP}}^f(W) &= \sigma_{C\text{-VP}}^f(W) + \sigma_{R\text{-VP}}^f(W) \\ &\quad + \sigma_{I\text{-VP}}^f(W),\end{aligned}\tag{15}$$

where

$$\begin{aligned}\sigma_{R\text{-VP}}^f(W) \equiv \sigma_R^f(W) &= \int_0^{1 - \left(\frac{W_{\text{min}}}{W}\right)^2} dx F(x, W) \\ &\quad \times \sigma_{B_R}^f(W\sqrt{1-x}),\end{aligned}\tag{16}$$

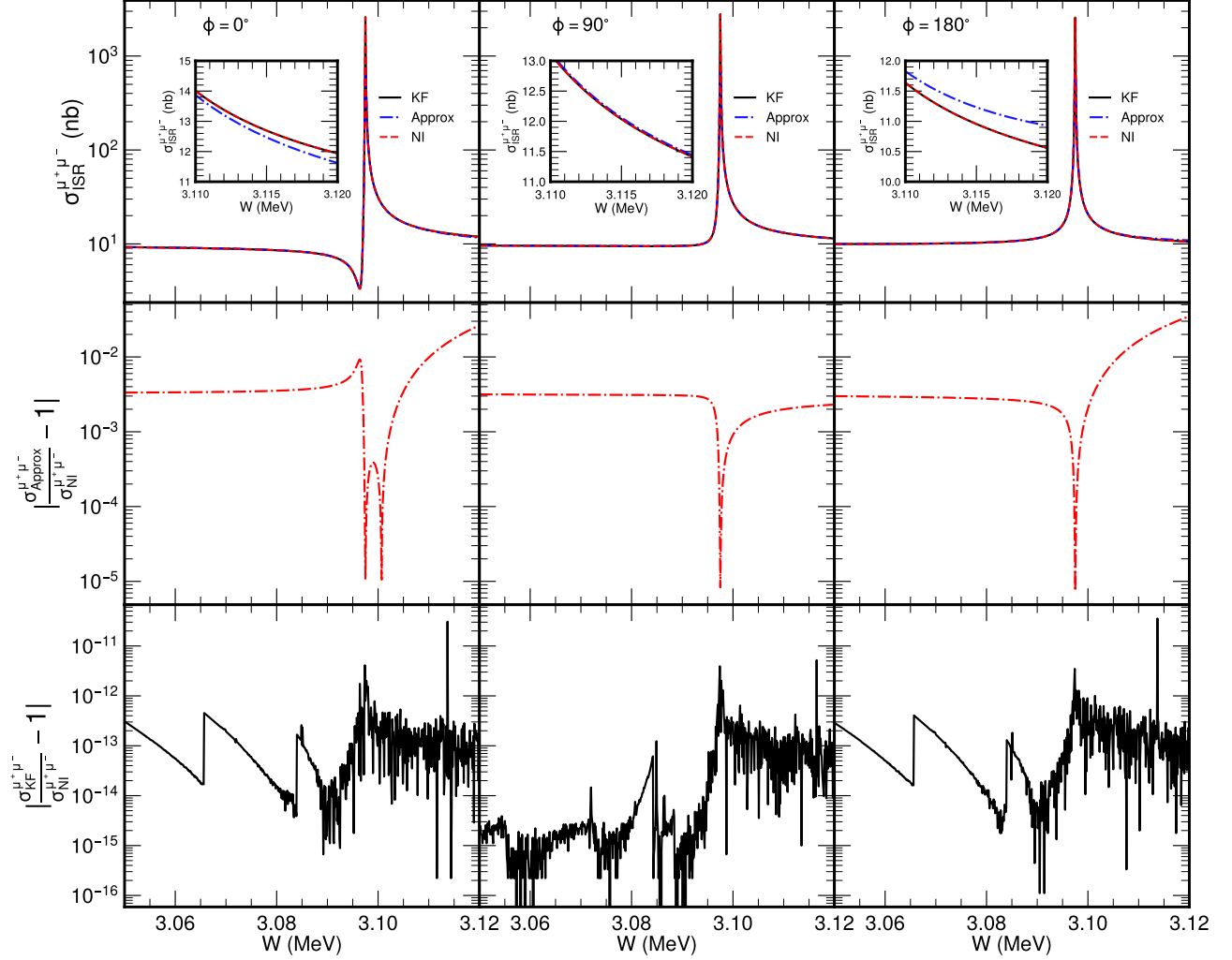


FIG. 1: The comparisons of ISR corrected cross sections for  $e^+e^- \rightarrow \mu^+\mu^-$  at  $\phi = 0^\circ$  at  $\phi = 0^\circ, 90^\circ$  and  $180^\circ$ . The Born cross section parameters are set to be PDG world averages [15] and  $W_{\min} = 2.0$  GeV. In the top row, black lines represent KF method results, blue dashed lines represent Approx method results and red dotted lines represent NI method results. In the middle row, red dashed lines represent the results of  $\left| \frac{\sigma_{\text{Approx}}^{\mu^+\mu^-}}{\sigma_{\text{NI}}^{\mu^+\mu^-}} - 1 \right|$ . In the bottom row, black lines represent the results of  $\left| \frac{\sigma_{\text{KF}}^{\mu^+\mu^-}}{\sigma_{\text{NI}}^{\mu^+\mu^-}} - 1 \right|$ .

$$\sigma_{C\text{-VP}}^f(W) \equiv \int_0^{1 - \left(\frac{W_{\min}}{W}\right)^2} dx F(x, W) \times \frac{\sigma_{BC}^f(W\sqrt{1-x})}{|1 - \Pi_0(W\sqrt{1-x})|^2}, \quad (17)$$

$$\simeq \frac{\sigma_C^f(W)}{|1 - \Pi_0(W)|^2}, \quad (18)$$



and

$$\sigma_{I\text{-VP}}^f(W) \equiv \int_0^{1-(\frac{W_{\min}}{W})^2} dx F(x, W) \times \frac{\sigma_{B_I}^f(W\sqrt{1-x})}{|1 - \Pi_0(W\sqrt{1-x})|}, \quad (19)$$

$$\simeq \frac{\sigma_I^f(W)}{|1 - \Pi_0(W)|}, \quad (20)$$

are integrals of the resonance, continuum, and interference contributions, respectively. Approximations are used in Eqs. (18) and (20) because the non-resonance VP factors  $\Pi_0(W)$  are numerically obtained [17].

In Fig. 2, we compare the ISR corrected cross section including VP effect  $\sigma_{\text{NI-VP}}^{\mu^+\mu^-}$  obtained through NI with  $\sigma_{\text{KF-VP}}^{\mu^+\mu^-}$  obtained using the KF analytic form and  $\sigma_{\text{Approx-VP}}^{\mu^+\mu^-}$  obtained using the approximated analytic form. The relative deviation between  $\sigma_{\text{NI-VP}}^{\mu^+\mu^-}$  and  $\sigma_{\text{Approx-VP}}^{\mu^+\mu^-}$  is at the order of  $10^{-4}$ , primarily arising from the simplifications made in Eq. (18) and (20). The deviation meets the 0.1% precision requirement of the SF method with corrections up to  $\mathcal{O}(\alpha^2)$  [7], thereby fulfilling the criteria for practical applicability. Furthermore, the relative deviation between  $\sigma_{\text{NI-VP}}^{\mu^+\mu^-}$  and  $\sigma_{\text{Approx-VP}}^{\mu^+\mu^-}$  remains about 0.3% at  $\phi = 90^\circ$ , and 3% at  $\phi = 0^\circ$  and  $180^\circ$ . It is evident that the precision of  $\sigma_{\text{Approx-VP}}^{\mu^+\mu^-}$  directly inherits from the one of  $\sigma_{\text{Approx}}^{\mu^+\mu^-}$ .

#### IV. C.M. ENERGY SPREAD EFFECT

For the narrow resonances, such as  $J/\psi$  whose decay width is 92.6 keV, the c.m. energy spreads of  $e^+e^-$  are much larger than the resonance widths. For example, the c.m. energy spread around  $J/\psi$  in BEPCII is less than 1 MeV [11]. Therefore, the effect for the c.m. energy spread must be considered in the experimentally observed cross section  $\sigma_{\text{exp}}^f(W)$  by a Gaussian convolution with  $\sigma_{\text{ISR-VP}}^f(W)$  which is

$$\sigma_{\text{ISR-exp}}^f(W) = \int_{W-n\delta_E}^{W+nS_E} \frac{1}{\sqrt{2\pi}S_E} \exp\left(-\frac{(W-W')^2}{2S_E^2}\right) \times \sigma_{\text{ISR-VP}}^f(W') dW'. \quad (21)$$

In Fig. 3, we compare ISR corrected cross sections including both the VP and c.m. energy spread effects  $\sigma_{\text{NI-exp}}^{\mu^+\mu^-}$  obtained through the NI with  $\sigma_{\text{KF-exp}}^{\mu^+\mu^-}$  obtained using the KF analytic

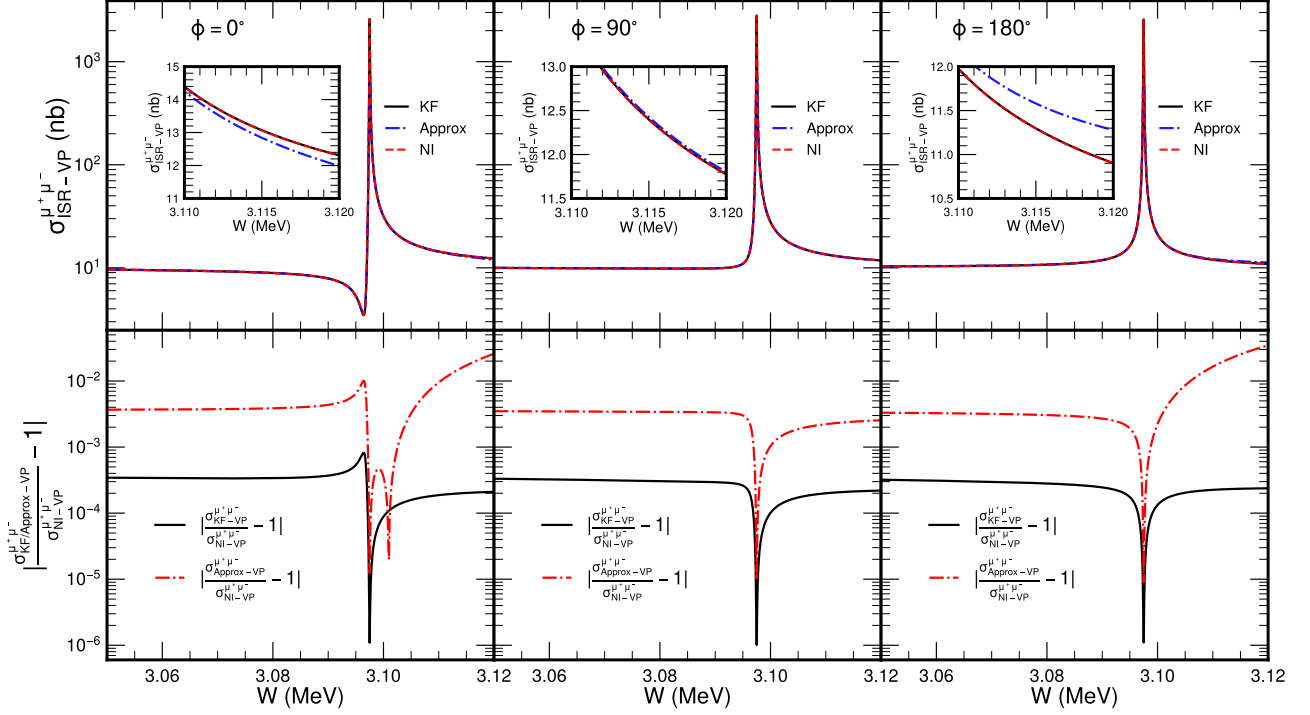


FIG. 2: The comparisons of ISR corrected cross sections with VP effect for  $e^+e^- \rightarrow \mu^+\mu^-$  at  $\phi = 0^\circ, 90^\circ$  and  $180^\circ$ . The Born cross section parameters are set to be PDG world averages [15] and  $W_{\min} = 2.0$  GeV. In the top row, black lines represent KF method results, blue dashed lines represent Approx method results and red dotted lines represent NI method results. In the bottom row, red dashed lines represent the results of  $\left| \frac{\sigma_{\text{Approx-VP}}^{\mu^+\mu^-}}{\sigma_{\text{NI-VP}}^{\mu^+\mu^-}} - 1 \right|$  and black lines represent the results of  $\left| \frac{\sigma_{\text{KF-VP}}^{\mu^+\mu^-}}{\sigma_{\text{NI-VP}}^{\mu^+\mu^-}} - 1 \right|$ .

form and  $\sigma_{\text{Approx-exp}}^{\mu^+\mu^-}$  obtained using the approximated analytic form. The relative deviation between  $\sigma_{\text{NI-exp}}^{\mu^+\mu^-}$  and  $\sigma_{\text{KF-exp}}^{\mu^+\mu^-}$  remains at the order of  $10^{-4}$ . Moreover, the relative deviation between  $\sigma_{\text{ISR-VP}}^{\text{NI}}$  and  $\sigma_{\text{ISR-VP}}^{\text{PE}}$  is still 0.3% at  $\Phi = 90^\circ$  and 3% at  $\Phi = 0^\circ$  and  $\Phi = 180^\circ$ . It is evident that the Gaussian convolution of the c.m. energy spread does not impact on the precision.

In Table I, we present a comparison of the consuming time for  $\sigma_{\text{KF-exp}}^f$ ,  $\sigma_{\text{Approx-exp}}^f$ , and  $\sigma_{\text{NI-exp}}^f$  for the processes  $e^+e^- \rightarrow \mu^+\mu^-$  and  $2(\pi^+\pi^-)\pi^0$ . Both the KF and approximated analytic forms significantly reduce the consuming time. Notably,  $\sigma_{\text{KF-exp}}^f$  yields the shortest computing time for the hadronic decay process.

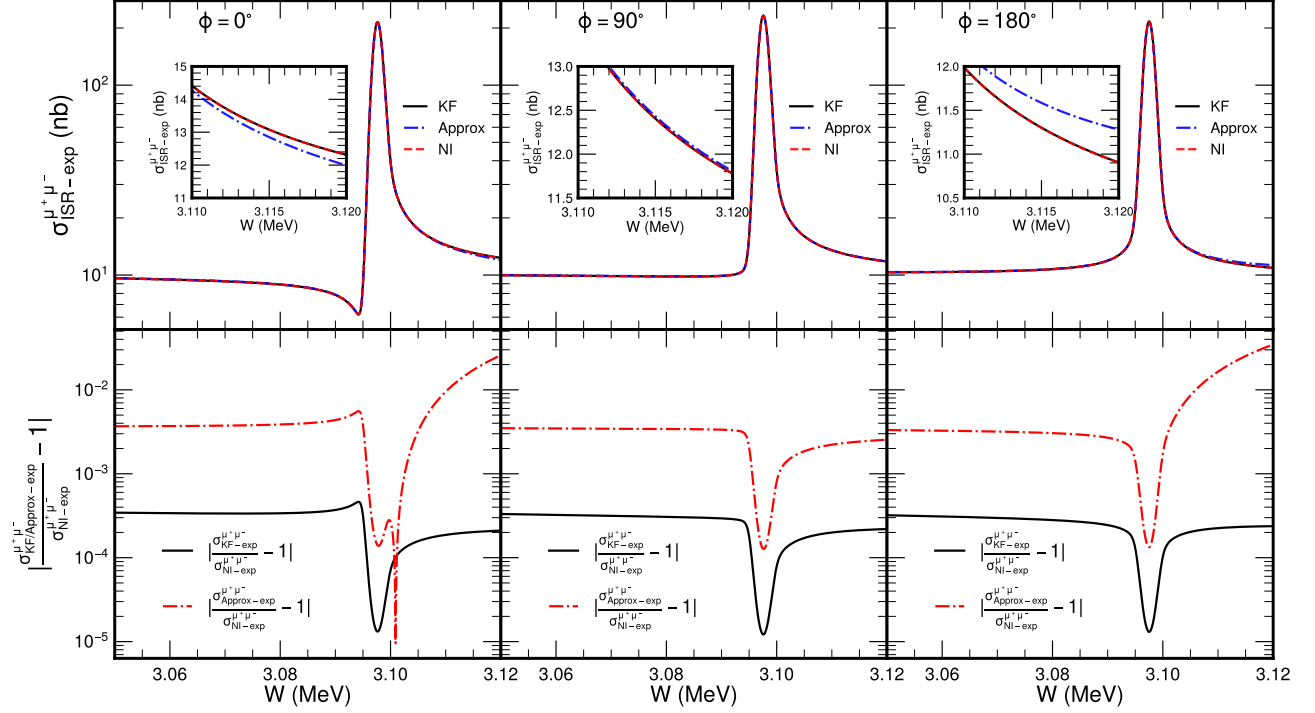


FIG. 3: The comparisons of ISR corrected cross section with VP effect and c.m. energy spread effect for  $e^+e^- \rightarrow \mu^+\mu^-$  at  $\phi = 0^\circ$  at  $\phi = 0^\circ, 90^\circ$  and  $180^\circ$ . The Born cross section parameters are set to be PDG world averages [15] and  $W_{\min} = 2.0$  GeV. In the top row, black lines represent KF method results, blue dashed lines represent Approx method results and red dotted lines represent NI method results. In the bottom row, red dashed lines represent the results of  $\left| \frac{\sigma_{\text{Approx-exp}}^{\mu^+\mu^-}}{\sigma_{\text{NI-exp}}^{\mu^+\mu^-}} - 1 \right|$  and black lines represent the results of  $\left| \frac{\sigma_{\text{KF-exp}}^{\mu^+\mu^-}}{\sigma_{\text{NI-exp}}^{\mu^+\mu^-}} - 1 \right|$ .

TABLE I: The comparison of the consuming times by parallel computation on 12 CPU cores within Python-based codes.

$N_{\text{points}}$	$e^+e^- \rightarrow \mu^+\mu^-$			$e^+e^- \rightarrow 5\pi$		
	$T_{\text{KF-exp}}(\text{s})$	$T_{\text{Approx-exp}}(\text{s})$	$T_{\text{NI-exp}}(\text{s})$	$T_{\text{KF-exp}}(\text{s})$	$T_{\text{Approx-exp}}(\text{s})$	$T_{\text{NI-exp}}(\text{s})$
10	0.18	0.13	9.90	0.15	0.59	15.24
100	0.48	0.34	32.59	0.34	2.06	50.73
1000	2.03	1.35	307.99	2.44	17.51	469.61

## V. FIT RESULTS USING TOY MC SAMPLES

We use the toy MC samples for  $e^+e^- \rightarrow \mu^+\mu^-$  and  $e^+e^- \rightarrow 2(\pi^+\pi^-)\pi^0$  around  $J/\psi$  to test our analytic form and compare it to the approximated one. Firstly, the toy MC samples for the ISR corrected cross sections of  $e^+e^- \rightarrow \mu^+\mu^-$  are generated with 1% uncertainty at 20 c.m. energies around  $J/\psi$ . The minimized  $\chi_{\mu^+\mu^-}^2$  is performed with the free parameters  $M$ ,  $S_E$  and  $\phi$ . The  $\chi_{\mu^+\mu^-}^2$  is Eq. (22)

$$\chi_{\mu^+\mu^-}^2(M, S_E, \phi) = \sum_{i=1}^{20} \left[ \frac{\sigma_i^{\mu^+\mu^-} - \sigma_{\text{ISR-exp}}^{\mu^+\mu^-}(W_i; M, S_E, \phi)}{\Delta\sigma_i^{\text{MC}}} \right]^2, \quad (22)$$

where  $\sigma_i^{\mu^+\mu^-}$  is the cross section at every energy point  $W_i$ ,  $\Delta\sigma_i^{\mu^+\mu^-}$  is the corresponding uncertainty. The estimators  $\widehat{M}$  and  $\widehat{S}_E$  and their corresponding uncertainties  $\sigma_{\widehat{M}}$  and  $\sigma_{\widehat{S}_E}$  are taken as the information of the  $e^+e^-$  collider.

Secondly, the toy MC samples for the ISR corrected cross sections of  $e^+e^- \rightarrow 2(\pi^+\pi^-)\pi^0$  are then generated with 1% uncertainty at the same 20 c.m. energies around  $J/\psi$ . The minimized  $\chi_{5\pi}^2$  is performed with the free parameters  $\mathcal{A}$ ,  $\mathcal{C}_2$  and  $\Phi$ , and the nuisance parameters  $\widehat{M}$  and  $\widehat{S}_E$ . Therefore, the estimators  $\widehat{\mathcal{A}}$ ,  $\widehat{\mathcal{C}}_2$  and  $\widehat{\Phi}$  can be obtained. The  $\chi_{5\pi}^2$  is Eq. (23)

$$\begin{aligned} \chi_{5\pi}^2(\mathcal{A}, \mathcal{C}_2, \Phi) = & \sum_{i=1}^{20} \left[ \frac{\sigma_i^{5\pi} - \sigma_{\text{ISR-exp}}^{5\pi}(W_i; \mathcal{A}, \mathcal{C}_2, \Phi, M, S_E)}{\Delta\sigma_i^{5\pi}} \right]^2 \\ & + \left( \frac{M - \widehat{M}}{\sigma_{\widehat{M}}} \right)^2 + \left( \frac{S_E - \widehat{S}_E}{\sigma_{\widehat{S}_E}} \right)^2. \end{aligned} \quad (23)$$

The branching fraction for  $J/\psi \rightarrow 2(\pi^+\pi^-)\pi^0$  satisfies [11]

$$\text{Br} = \left( \frac{\mathcal{A}}{W^2} \right)^2 \Gamma_{\mu\mu} |(1 + \mathcal{C}_2 e^{i\Phi})|^2. \quad (24)$$

Finally, the above toy MC sample generations and  $\chi^2$  minimizations are repeated 10000 times. The fit results of  $e^+e^- \rightarrow \mu^+\mu^-$  are shown in Fig. 4. The estimators of  $\widehat{M}$  and  $\widehat{S}_E$  are centered around the MC truth values for both KF and approximated analytic forms. Only the estimator  $\widehat{\phi}$  of the KF analytic form is centered around the MC truth value. While the distribution of the estimator  $\widehat{\phi}$  of the approximated analytic form deviate more than  $2\sigma$  from the MC truth value. The  $\chi_{\mu^+\mu^-}^2$  of the KF analytic form is better than that of the approximated analytic form.

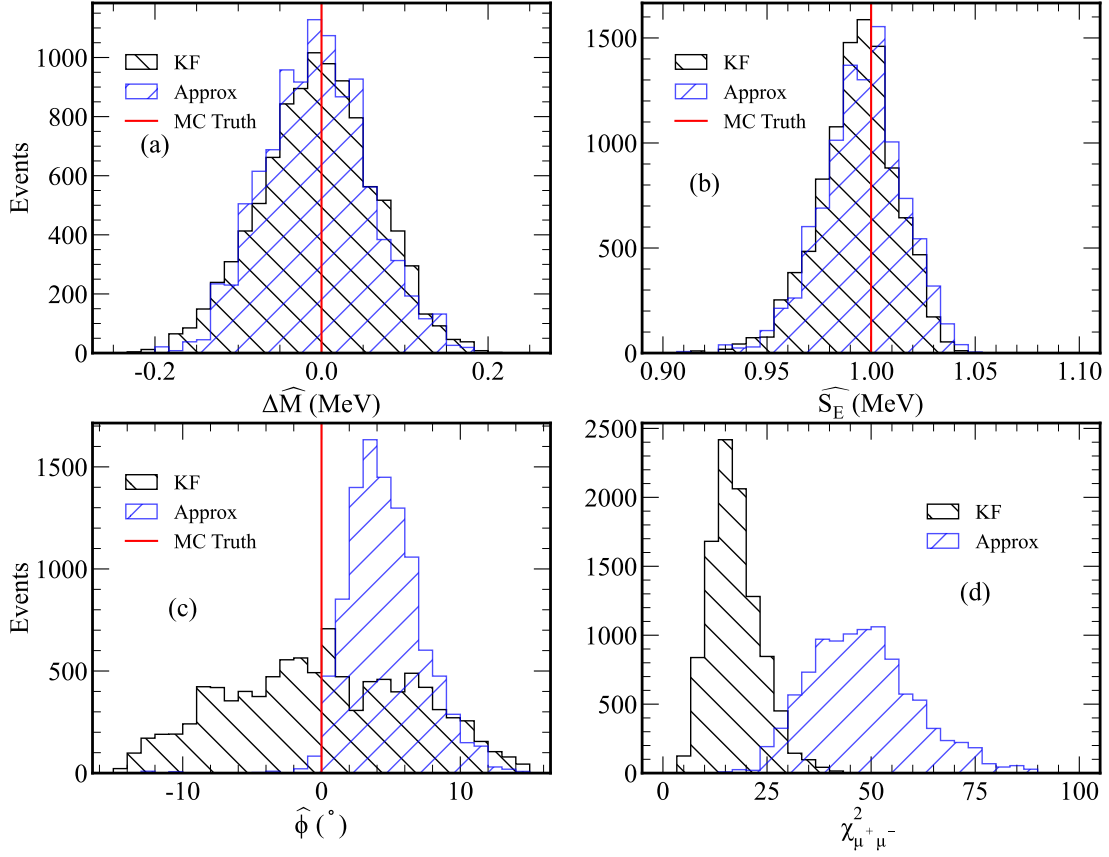


FIG. 4: The histograms of the estimators obtained from toy MC samples for  $e^+e^- \rightarrow \mu^+\mu^-$ . (a), (b), (c) and (d) show the distributions of  $\Delta\widehat{M} = \widehat{M} - M_{J/\psi}^{\text{MC Truth}}$ ,  $\widehat{S}_E$ ,  $\widehat{\phi}$  and  $\chi_{\mu^+\mu^-}^2$ , respectively. Histograms with black edges represent the KF analytic form, blue edges represent Approx analytic form and red lines are the values of MC truth.

The fit results for the process  $e^+e^- \rightarrow 2(\pi^+\pi^-)\pi^0$  are depicted in Fig. 5. Two solutions, labeled as Solution I and II, are obtained. The distributions of  $\chi_{5\pi}^2$  are identical for both Solution I and II. The  $\chi_{5\pi}^2$  of the KF analytic form is better than that of the approximated analytic form. Only in Solution I the estimator  $\widehat{\Phi}$  is centered around the MC truth value of  $90^\circ$ . While in Solution II,  $\widehat{\Phi}$  is centered around  $-90^\circ$ . Furthermore, in Solution I, only the estimator  $\widehat{\text{Br}}$  of the KF analytic form is centered around the MC truth value, whereas the estimator of the approximated analytic form deviates significantly. The toy MC test shows that the KF analytic form avoids a subtle yet non-negligible uncertainty that arises from

employing the approximated analytic form.

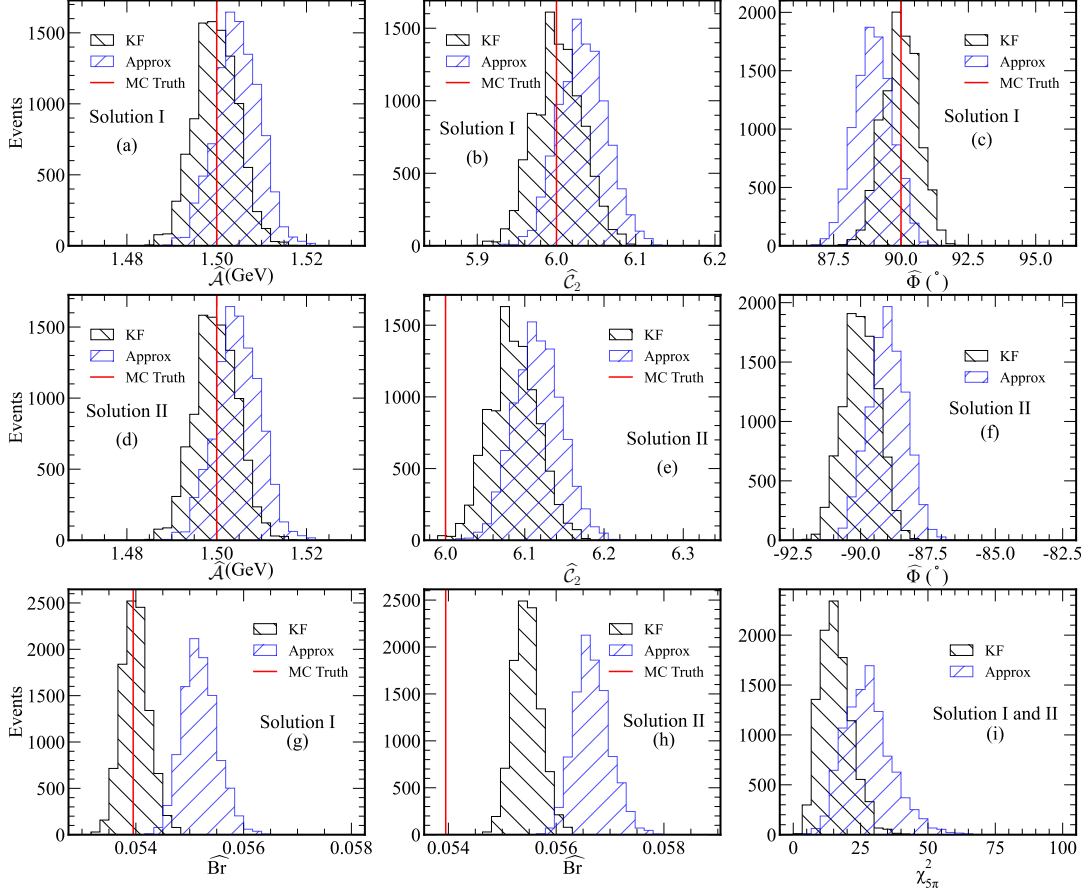


FIG. 5: The histograms of the estimators obtained from toy MC samples for  $e^+e^- \rightarrow 2(\pi^+\pi^-)\pi^0$ . (a), (b), (c) and (g) show the distributions of  $\widehat{\mathcal{A}}$ ,  $\widehat{\mathcal{C}}_2$ ,  $\widehat{\Phi}$  and  $\widehat{\text{Br}}$  for Solution I, respectively; (d), (e), (f) and (h) show the distributions of  $\mathcal{A}$ ,  $\mathcal{C}_2$ ,  $\Phi$  and  $\widehat{\text{Br}}$  for Solution II, respectively; (i) shows  $\chi^2_{5\pi}$  distributions for both Solution I and II. Histograms with black edges represent the KF analytic form, blue edges represent Approx analytic form and red lines are the values of MC truth.

## VI. DISCUSSIONS AND CONCLUSIONS

The ISR correction is essential for precise cross section measurements in  $e^+e^-$  annihilation. The structure functions method provides an integral transformation from the Born cross sections to the experimentally observed ones. For the first time, we present the exact analytic form for the ISR corrected cross section around a resonance with the KF radiative function. Even including the vacuum polarization (VP) and c.m. energy spread effects, the precision remains matches the accuracy requirement of the structure functions (SF) method up to  $\mathcal{O}(\alpha^2)$  [7]. The analytic form can accelerate the regression procedure used to extract physical parameters, such as the branching fraction, by over 150 times. Utilizing the toy MC samples, we reveal a non-negligible few percent systematic uncertainty caused by the approximated analytic form.

For the currently running  $e^+e^-$  collision experiments, the BESIII experiment has been accumulated 10 billion  $J/\psi$  events [18] and 3 billion  $\psi(3686)$  events [19] which are at least 6 times larger than those used in previous BESIII measurements. Furthermore, the Belle II experiment plans to take about  $500 \text{ fb}^{-1}$  data for each vector bottomonium state [20] which are at least ten or hundreds of times larger than the Belle experiment. The KF analytic form will be helpful to handle the ISR correction properly in currently running experiments at BESIII and Belle II, as well as in planned ones, such as the super-tau-charm factories (STCF) [21] and the super- $J/\psi$  factory [22].

## ACKNOWLEDGMENTS

X. Z. would like to acknowledge useful conversations with Y. D. Wang and K. Zhu. This work has been supported by the National Natural Science Foundation of China (NSFC) under Contract Nos. U2032114 and 12192265).

## Appendix A: Analytic forms for Born Cross Sections

The Born cross section of the process  $e^+e^- \rightarrow \mu^+\mu^-$  is [11]

$$\sigma_{\text{Born}}^{\mu^+\mu^-}(W) = \frac{4\pi\alpha^2}{3W^2} \left| 1 + \frac{W^2}{M} \times \frac{3\sqrt{\Gamma_{ee}\Gamma_{\mu\mu}}}{\alpha(W^2 - M^2 + iM\Gamma)} e^{i\phi} \right|^2, \quad (\text{A1})$$

which can be taken apart into three parts

$$\sigma_{B_c}^{\mu^+\mu^-}(W) = \frac{4\pi\alpha^2}{3W^2}, \quad (\text{A2})$$

$$\sigma_{B_R}^{\mu^+\mu^-}(W) = \frac{12\pi W^2 \Gamma_{ee} \Gamma_{\mu\mu}}{M^2((W^2 - M^2)^2 + M^2\Gamma^2)}, \quad (\text{A3})$$

$$\sigma_{B_I}^{\mu^+\mu^-}(W) = \frac{8\pi\alpha\sqrt{\Gamma_{ee}\Gamma_{\mu\mu}}}{M((W^2 - M^2)^2 + M^2\Gamma^2)} \times ((W^2 - M^2)\cos\phi + M\Gamma\sin\phi). \quad (\text{A4})$$

The Born cross section of the process  $e^+e^- \rightarrow 2(\pi^+\pi^-)\pi^0$  is [11]

$$\sigma_{\text{Born}}^{5\pi}(W) = \left( \frac{\mathcal{A}}{W^2} \right)^2 \frac{4\pi\alpha^2}{3W^2} \left| 1 + \frac{W^2}{M} \times \frac{3\sqrt{\Gamma_{ee}\Gamma_{\mu\mu}}\mathcal{C}_1 e^{i\phi} (1 + \mathcal{C}_2 e^{i\Phi})}{\alpha(W^2 - M^2 + iM\Gamma)} \right|^2, \quad (\text{A5})$$

which can also be taken apart into three parts:

$$\sigma_{B_c}^{5\pi}(W) = \left( \frac{\mathcal{A}}{W^2} \right)^2 \frac{4\pi\alpha^2}{3W^2}, \quad (\text{A6})$$

$$\sigma_{B_R}^{5\pi}(W) = \mathcal{C}_1^2(1 + \mathcal{C}_2^2 + 2\mathcal{C}_2\cos\Phi) \times \frac{12\pi\mathcal{A}^2\Gamma_{ee}\Gamma_{\mu\mu}}{M^2W^2((W^2 - M^2)^2 + M^2\Gamma^2)}, \quad (\text{A7})$$

$$\sigma_{B_I}^{5\pi}(W) = \frac{8\pi\alpha\mathcal{A}^2\sqrt{\Gamma_{ee}\Gamma_{\mu\mu}}}{W^4M((W^2 - M^2)^2 + M^2\Gamma^2)} \times [(W^2 - M^2)\mathcal{C}_1(\cos\phi + \mathcal{C}_2\cos\phi\cos\Phi - \mathcal{C}_2\sin\phi\sin\Phi) + M\Gamma\mathcal{C}_1(\sin\phi + \mathcal{C}_2\cos\phi\sin\Phi + \mathcal{C}_2\sin\phi\cos\Phi)]. \quad (\text{A8})$$



## Appendix B: Analytic forms of ISR corrected cross sections

The ISR corrected cross section from the continuum part of  $e^+e^- \rightarrow \mu^+\mu^-$  is

$$\sigma_C^{\mu^+\mu^-} = \frac{4\pi\alpha^2}{3W^2} I_0. \quad (\text{B1})$$

The ISR corrected cross section from the resonance part of  $e^+e^- \rightarrow \mu^+\mu^-$  is

$$\begin{aligned} \sigma_R^{\mu^+\mu^-} &= \frac{6\pi\Gamma_{ee}\Gamma_{\mu\mu}W^2}{M^5\Gamma} \left[ \left(1 + \frac{A}{B}\right) I_1 - \frac{1}{B} I_2 \right] \\ &+ \text{c.c..} \end{aligned} \quad (\text{B2})$$

The ISR corrected cross section from the interference part of  $e^+e^- \rightarrow \mu^+\mu^-$  is

$$\begin{aligned} \sigma_I^{\mu^+\mu^-} &= \left[ \frac{4\pi\alpha\sqrt{\Gamma_{ee}\Gamma_{\mu\mu}}}{M^3\Gamma} (\Gamma\sin\phi - M\cos\phi) + \right. \\ &\quad \left. \frac{4\pi\alpha\sqrt{\Gamma_{ee}\Gamma_{\mu\mu}}W^2\cos\phi}{M^4\Gamma} \left(1 + \frac{A}{B}\right) \right] I_1 \\ &\quad - \frac{I_2W^2}{B} \frac{4\pi\alpha\sqrt{\Gamma_{ee}\Gamma_{\mu\mu}}}{M^4\Gamma} \cos\phi + \text{c.c..} \end{aligned} \quad (\text{B3})$$

The ISR corrected cross section from the continuum part of  $e^+e^- \rightarrow 2(\pi^+\pi^-)\pi^0$  is

$$\sigma_C^{5\pi} = \frac{4\pi\alpha^2\mathcal{A}^2}{3W^6} I_3. \quad (\text{B4})$$

The ISR corrected cross section from the resonance part of  $e^+e^- \rightarrow 2(\pi^+\pi^-)\pi^0$  is

$$\begin{aligned} \sigma_R^{5\pi} &= \mathcal{C}_1^2(1 + \mathcal{C}_2^2 + 2\mathcal{C}_2\cos\Phi) \frac{6\pi\mathcal{A}^2\Gamma_{ee}\Gamma_{\mu\mu}}{\Gamma M^5W^2} \\ &\quad \left( \frac{1}{A+B} I_0 + \frac{B}{A+B} I_1 \right) + \text{c.c..} \end{aligned} \quad (\text{B5})$$

The ISR corrected cross section from the interference part of  $e^+e^- \rightarrow 2(\pi^+\pi^-)\pi^0$  is

$$\begin{aligned} \sigma_I^{5\pi} &= \frac{4\pi\alpha\mathcal{A}^2\sqrt{\Gamma_{ee}\Gamma_{\mu\mu}}}{M} \left\{ \left[ \frac{\mathcal{C}_1}{W^4M^2} \right. \right. \\ &\quad \times (\sin\phi + \mathcal{C}_2\cos\phi\sin\Phi + \mathcal{C}_2\sin\phi\cos\Phi) \\ &\quad \left. - \frac{\mathcal{C}_1(\cos\phi + \mathcal{C}_2\cos\phi\cos\Phi - \mathcal{C}_2\sin\phi\sin\Phi)}{\Gamma W^4M} \right] \\ &\quad \times \left[ \frac{B}{(A+B)^2} I_0 + \left( \frac{B}{A+B} \right)^2 I_1 + \frac{1}{A+B} I_4 \right] + \\ &\quad \left. \frac{\mathcal{C}_1(\cos\phi + \mathcal{C}_2\cos\phi\cos\Phi - \mathcal{C}_2\sin\phi\sin\Phi)}{\Gamma W^2M^3} \left( \frac{1}{A+B} I_0 \right. \right. \\ &\quad \left. \left. + \frac{B}{A+B} I_1 \right) \right\} + \text{c.c..} \end{aligned} \quad (\text{B6})$$

where c.c. represents the complex conjugate of the former part,  $A = \frac{\Gamma}{M} + i \left[ \left( \frac{W}{M} \right)^2 - 1 \right]$ ,  $B = -i \left( \frac{W}{M} \right)^2$  and  $b = 1 - \left( \frac{W_{\min}}{W} \right)^2$ . The five integrations  $I_0$ ,  $I_1$ ,  $I_2$ ,  $I_3$  and  $I_4$  are

$$I_0 = \beta(1 + \delta) \mathcal{B}(b, \beta, 0) - \frac{b\beta}{2} + \log(1 - b) \left( \frac{1}{4}\beta^2 + \frac{\beta}{2} + \frac{3}{8}\beta^2 b \right) + \frac{1}{16}\beta^2 \log^2(1 - b) - \frac{\beta^2}{2} b \log b - \frac{\beta^2}{2} \left( \text{Li}_2(1 - b) - \frac{\pi^2}{6} - \text{Li}_2(b) \right). \quad (\text{B7})$$

$$I_1 = \beta(1 + \delta) \left( \frac{b^\beta {}_2F_1(1, \beta, 1 + \beta, -bB/A)}{A\beta} \right) + \left( \frac{\beta^2}{8} + \frac{\beta}{2} \right) \left( \frac{b}{B} - \frac{A}{B^2} \log \frac{A + Bb}{A} \right) - \left( \beta + \frac{3}{4}\beta^2 \right) \frac{1}{B} \log \frac{A + Bb}{A} + \frac{3}{4}\beta^2 \left[ -\frac{1}{B} \left[ \text{Li}_2 \left( \frac{A + Bb}{A + B} \right) - \text{Li}_2 \left( \frac{A}{A + B} \right) + \log \frac{B}{A + B} \log \frac{A + Bb}{A} \right] \right] - \frac{3}{8}\beta^2 \frac{1}{B} [-b + (b - 1) \log(1 - b) + \frac{A}{B} \left[ \text{Li}_2 \left( \frac{A + Bb}{A + B} \right) - \text{Li}_2 \left( \frac{A}{A + B} \right) + \log \frac{B}{A + B} \log \frac{A + Bb}{A} \right]] - \beta^2 \frac{1}{B} \left[ -\frac{\pi^2}{6} + \frac{1}{2} \log^2 \left( 1 + \frac{B}{A} b \right) + \text{Li}_2 \left( \frac{A}{A + Bb} \right) - \log \frac{B}{A} \log \left( 1 + \frac{B}{A} b \right) \right] + \frac{1}{2}\beta^2 \frac{1}{B} \left[ b(\log b - 1) - \frac{A}{B} \left[ -\frac{\pi^2}{6} + \frac{1}{2} \log^2 \left( 1 + \frac{B}{A} b \right) + \text{Li}_2 \left( \frac{A}{A + Bb} \right) - \log \frac{B}{A} \log \left( 1 + \frac{B}{A} b \right) \right] \right] - \frac{1}{2}\beta^2 \frac{1}{A} \left[ -\text{Li}_2(b) + \left[ \text{Li}_2 \left( \frac{A + Bb}{A + B} \right) - \text{Li}_2 \left( \frac{A}{A + B} \right) + \log \frac{B}{A + B} \log \frac{A + Bb}{A} \right] \right], \quad (\text{B8})$$

$$I_2 = \beta(1 + \delta) \frac{b^\beta}{\beta} + \frac{\beta^2}{2} \text{Li}_2(b) + b^2 \left( \frac{\beta}{4} + \frac{1}{32}\beta^2 \right) + b \left( -\beta - \frac{5}{16}\beta^2 \right) + \log(1 - b) \left( -\frac{9}{16}\beta^2 + \frac{3}{4}\beta^2 b - \frac{3}{16}\beta^2 b^2 \right) + \log b \left( \frac{\beta^2 b^2}{4} - \beta^2 b \right), \quad (\text{B9})$$

$$I_3 = \beta(1 + \delta) \mathcal{B}(b, \beta, -2) + \left( \frac{\beta^2}{8} + \frac{\beta}{2} \right) \frac{-1 + (1 - b)^3 + b(b + 3 - 3b)}{2(1 - b)^3} - \frac{1}{2} \left( \beta + \frac{3}{4}\beta^2 \right) \left( \frac{1}{(1 - b)^2} - 1 \right) - \frac{\beta^2}{8} \frac{1 - (1 - b)^2 + 2 \log(1 - b)}{4(1 - b)^2} - \frac{3}{4}\beta^2 \log(1 - b) - \frac{\beta^2}{4} \frac{b(b - 1 - (b - 2) \log b)}{(1 - b)^2} + \frac{\beta^2}{2} \frac{b \log b}{b - 1} - \frac{1}{2}\beta^2 \left( -\text{Li}_2(b) - \frac{1}{2} \log^2(1 - b) \right) - \frac{\beta}{8} \frac{b + \log(1 - b)}{1 - b}, \quad (\text{B10})$$

and

$$I_4 = \beta(1 + \delta)\mathcal{B}(b, \beta, -1) + \frac{\beta^2}{2}(\text{Li}_2(b) - \text{Li}_2(1 - b) + \frac{\pi^2}{6}) + \frac{b}{1 - b} \left( -\frac{3}{4}\beta^2 - \frac{\beta}{2} \right) + \log(1 - b) \left( \frac{\beta}{2} - \frac{3}{8}\beta^2 \right) - \frac{b \log b \beta^2}{1 - b} + \log^2(1 - b) \frac{\beta^2}{16} - \frac{\beta^2 \log(1 - b)}{8(1 - b)}. \quad (\text{B11})$$

The special functions used in the above formulas are

$$\text{Li}_2 = - \int_0^z \frac{\log(1 - u)}{u} du, \quad (\text{B12})$$

$$\mathcal{B}(x, a, b) = \int_0^x t^{a-1}(1 - t)^{b-1} dt, \quad (\text{B13})$$

and

$${}_2F_1(a, b, c, x) = \sum_{n=0}^{\infty} \frac{(a)_n (b)_n}{(c)_n} \frac{x^n}{n!}, \quad (\text{B14})$$

where  $\text{Li}_2$  is the Spence function,  $\mathcal{B}$  is the beta function and  ${}_2F_1$  is the Gaussian hypergeometric function with the Pochhammer symbol  $(a)_n = \Gamma(a + n)/\Gamma(a)$  and  $\Gamma(x)$  is the Gamma function.

- 
- [1] N. Brambilla *et al.*, Heavy quarkonium: progress, puzzles, and opportunities, *Eur. Phys. J. C* **71**, 1534 (2011).
  - [2] P. Wang, C. Z. Yuan, X. H. Mo, and D. H. Zhang, The interference between virtual photon and  $1^{--}$  charmonium in  $e^+e^-$  experiment, *Phys. Lett. B* **593**, 89 (2004).
  - [3] P. Wang, X. H. Mo, and C. Z. Yuan, Measurement of the exclusive light hadron decays of the  $\psi''$  in  $e^+e^-$  experiments, *Int. J. Mod. Phys. A* **21**, 5163 (2006).
  - [4] Y. P. Guo and C. Z. Yuan, Impact of the interference between the resonance and continuum amplitudes on vector quarkonia decay branching fraction measurements, *Phys. Rev. D* **105**, 114001 (2022).
  - [5] S. Actis *et al.*, Quest for precision in hadronic cross sections at low energy: Monte carlo tools vs. experimental data, *Eur. Phys. J. C* **66**, 585 (2010).
  - [6] X. K. Dong, L. L. Wang, and C. Z. Yuan, Derived Born cross sections of  $e^+e^-$  annihilation into open charm mesons from CLEO-c measurements, *Chin. Phys. C* **40**, 043002 (2018).
  - [7] E. A. Kuraev and V. S. Fadin, On radiative corrections to the cross section for single photon annihilation of an  $e^+e^-$  pair at high energy, *Sov. J. Nucl. Phys.* **41**, 466 (1985).

- [8] W. Y. Sun, T. Liu, M. Q. Jing, B. Zhong, and W. M. Song, An iterative weighting method to apply isr correction to  $e^+e^-$  hadronic cross-section measurements, *Frontiers of Physics* **16**, 64501 (2021).
- [9] S. S. Gribov and A. S. Popov, A new method for obtaining a born cross section using visible cross section data from  $e^+e^-$  colliders, *J. High Energ. Phys.* **11**, 203 (2021).
- [10] Y. D. Wang, Y. N. Wang, and P. Wang, Analytical formula for the cross section of hadron production from  $e^+e^-$  collisions around the narrow charmonium resonances, arXiv 10.48550/arXiv.2311.13292 (2023).
- [11] M. Ablikim *et al.* (BESIII Collaboration), Measurement of the phase between strong and electromagnetic amplitudes of  $J/\psi$  decays, *Physics Letter B.* **791**, 375 (2019).
- [12] R. N. Cahn, Analytic forms for the  $e^+e^-$  annihilation cross section near the X including initial-state radiation, *Phys. Rev. D* **36**, 2666 (1987).
- [13] F. Z. Chen, P. Wang, J. M. Wu, and Y. S. Zhu, Radiative correction of the resonant cross section in  $e^+e^-$  collision, *Chin. Phys. C* **14**, 585 (1990).
- [14] X. Y. Zhou, Y. D. Wang, and L. G. Xia, Analytic forms for cross sections of di-lepton production from  $e^+e^-$  collisions around the  $J/\psi$  resonance, *Chinese Phys. C* **41**, 083001 (2017).
- [15] R. L. Workman *et al.* (Particle Data Group), Review of particle physics, *Prog. Theor. Exp. Phys.* **2022**, 083C01 (2022).
- [16] V. V. Anashin *et al.* (KEDR collaboration), Measurement of  $\Gamma_{ee}(J/\psi) \cdot \mathcal{B}(J/\psi \rightarrow e^+e^-)$  and  $\Gamma_{ee}(J/\psi) \cdot \mathcal{B}(J/\psi \rightarrow \mu^+\mu^-)$ , *Phys. Lett. B* **711**, 280 (2012).
- [17] A. Blondel, J. Gluza, S. Jadach, P. Janot, and T. Riemann, eds., *Theory for the FCC-ee: Report on the 11th FCC-ee Workshop Theory and Experiments*, CERN Yellow Reports: Monographs, Vol. 3/2020 (CERN, Geneva, 2019).
- [18] M. Ablikim *et al.* (BESIII Collaboration), Number of  $J/\psi$  events at BESIII, *Chin. Phys.C* **46**, 074001 (2021).
- [19] M. Ablikim *et al.* (BESIII Collaboration), Determination of the number of  $\psi(3686)$  events taken at BESIII, arXiv: 10.48550/arXiv.2403.06766 (2024).
- [20] E. Kou *et al.* (Belle II Collaboration), The Belle II Physics Book, *Prog. Theor. Exp. Phys.* **2019**, 123C01 (2019).
- [21] H. P. Peng, Y. H. Zhen, and X. R. Zhou, Super tau-charm facility of china, *Physics* **49**, 8 (2020).

- [22] C. Z. Yuan and M. Karliner, Cornucopia of Antineutrons and Hyperons from a Super  $J/\psi$  Factory for Next-Generation Nuclear and Particle Physics High-Precision Experiments, Phys. Rev. Lett. **127**, 012003 (2021).